



## Evapotranspiration and biomass modelling in the Pontal Sul Irrigation Scheme

Leandro Moscôso Araujo, Antônio Heriberto de Castro Teixeira & Luís Henrique Basso

To cite this article: Leandro Moscôso Araujo, Antônio Heriberto de Castro Teixeira & Luís Henrique Basso (2020) Evapotranspiration and biomass modelling in the Pontal Sul Irrigation Scheme, International Journal of Remote Sensing, 41:6, 2326-2338, DOI: [10.1080/01431161.2019.1688416](https://doi.org/10.1080/01431161.2019.1688416)

To link to this article: <https://doi.org/10.1080/01431161.2019.1688416>



Published online: 12 Nov 2019.



Submit your article to this journal [↗](#)



Article views: 106



View related articles [↗](#)



View Crossmark data [↗](#)



# Evapotranspiration and biomass modelling in the Pontal Sul Irrigation Scheme

Leandro Moscôso Araujo <sup>a</sup>, Antônio Heriberto de Castro Teixeira<sup>a,b</sup>  
and Luís Henrique Basso<sup>a,c</sup>

<sup>a</sup>Graduate Program in Agronomy/Irrigation and Drainage, Department of Rural Engineering, São Paulo State University/UNESP, Botucatu, Brazil; <sup>b</sup>Federal University of Sergipe/PRORH, Aracaju, Brazil; <sup>c</sup>Embrapa Instrumentation, São Carlos, Brazil

## ABSTRACT

In order to make feasible the use of irrigated areas of the Pontal Sul Irrigation Scheme in Petrolina, State of Pernambuco, Brazil, modelling of real evapotranspiration (ET) and plant biomass production (BIO) at a large scale was performed with associated agrometeorological data and the algorithm SAFER (*Simple Algorithm For Evapotranspiration Retrieving*) using MODIS images for the years 2010–2017. The year 2012 presented the highest ET average with 3.15 mm day<sup>-1</sup> in the rainy season, reaching a maximum of 6 mm day<sup>-1</sup>. The lowest mean ET was recorded in the year 2013, with 0.08 mm day<sup>-1</sup> in the dry season, and the maximum recorded for the period was 3.40 mm day<sup>-1</sup> in the irrigated agricultural area. For BIO, the highest average was 104.82 kg ha<sup>-1</sup> day<sup>-1</sup>, during the rainy season of 2012, reaching a maximum value of 252 kg ha<sup>-1</sup> day<sup>-1</sup>. The lowest average was for the dry period of 2013, with a value of 0.93 kg ha<sup>-1</sup> day<sup>-1</sup>, and a maximum of 112.51 kg ha<sup>-1</sup> day<sup>-1</sup> in the irrigated agricultural area. The higher ET results represent moisture in the root zone, provided by rainfall and/or irrigation, showing maximum values in the rainy season. The results obtained for BIO suffer greatly from perimeter water availability. The present study becomes very important to the management of water resources, as it provides an increase in water productivity for food production.

## ARTICLE HISTORY

Received 21 March 2019

Accepted 19 September 2019

## 1. Introduction

Irrigated agriculture is an important economic activity in Northeastern Brazil, but as its area expands, so do the demands for greater agricultural production and rational water usage. However, the low, irregularly-distributed rainfall and the high evapotranspiration rates in the region restrict water availability, necessitating the rational use of water while increasing agricultural production.

Large-scale evapotranspiration (ET) modelling using satellite imagery and based on the climatic conditions of each region and the water needs of the planted crops becomes very important to irrigation management plans aimed at increasing the efficiency of water

**CONTACT** Leandro Moscôso Araujo  [leandro\\_moscoso@hotmail.com](mailto:leandro_moscoso@hotmail.com)  Graduate Program in Agronomy/Irrigation and Drainage, Department of Rural Engineering, São Paulo State University/UNESP, Botucatu, São Paulo, Brazil

resource usage. ET quantification is a crucial in agricultural water management and in hydrological modelling, enabling measurement of the water available for human and ecological consumption (Shekar and Nandagiri 2016). However, its estimation needs to be precise, obtained operationally, based on physical principles, and encompass wide areas in order to meet the information requirements that assist in the management of water resources (Cleugh et al. 2007).

According to de Castro Teixeira et al. (2013a), ET is an important precursor in the quantification of plant biomass production (BIO), both for agricultural and native vegetation areas, as these parameters are indicative of hydric and vegetation conditions.

The municipality of Petrolina, in Pernambuco state, stands out as an important agricultural centre due to the irrigation technologies applied to fruit crops in the vicinity of the São Francisco River (de Castro Teixeira et al. 2017a, 2017b). Although the large-scale energy balance developed in this municipality has already been the subject of previous studies (de Castro Teixeira et al. 2013a, 2013b, 2017a, 2017b), more specific research on the quantification of water productivity (WP) components, such as ET and local BIO, still needs to be carried out to improve usage planning in irrigated areas in the Pontal Sul Irrigated Scheme.

Thus, the objective of the present study consisted of monitoring the different agroecosystems of the Pontal Sul Irrigated Scheme between 2010 and 2017 by modelling ET and BIO on a large scale using remote sensing techniques, interpolating and associating data from agro-meteorological stations to the SAFER (Simple Algorithm For Evapotranspiration Retrieving) algorithm, and combining images from the MODIS sensor with the climatic conditions of the Pernambuco semi-arid region.

## 2. Material and methods

Figure 1 shows the exact location of the Pontal Sul Irrigation Scheme within the municipality of Petrolina (PE), delimited between the geographic coordinates 8°55'39.66"S and 40°38'13.39"W (in the upper region) and 9°07'33.20"S and 40°25'47.45" W, as well as irrigated agricultural areas and the agro-meteorological stations from which climatic data were used for the period between 2010 and 2017.

Global solar radiation ( $R_G$ ), air temperature ( $T_a$ ), relative air humidity (RH), and wind speed ( $u$ ) were used to estimate the large-scale evapotranspiration reference ( $ET_0$ ) via the Penman-Monteith method (Allen et al. 1998).

Rainfall data ( $P$ ) were used to characterize the following seasons: rainy season (January–April), end of the rainy season (May–July), dry season (September–October), and beginning of the rainy season (November–December) in the irrigation scheme area.

The local climate is classified as BSw' according to Köppen's climate scale, being a semi-arid region (Teixeira 2012), with an annual average rainfall below 600 mm, concentrated between the months of January and March, and an unstable water deficit lasting between 8 and 10 months; the average air temperature varies between 24 and 28°C.

The native vegetation that predominates in the region is the Caatinga, with characteristic shrub species morphology: small leaves, thorns, and deep roots, providing greater tolerance to the water deficit (de Souza et al. 2015). In the Pontal Sul Irrigation Scheme, part of the native vegetation will be replaced by irrigated agriculture. This project was developed by the Vales do São Francisco e do Parnaíba Development Company (CODEVASF), and includes

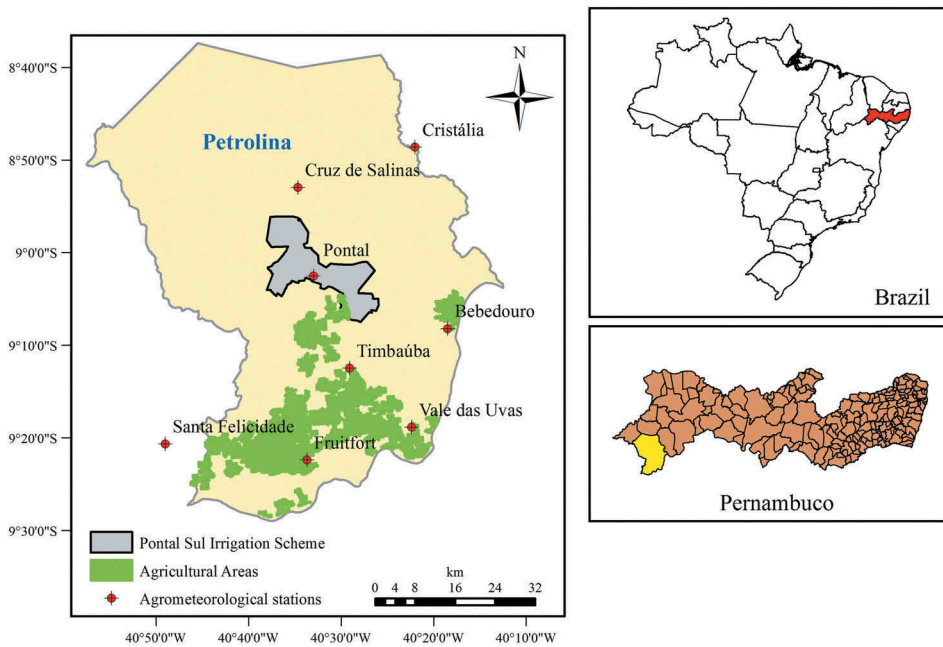


**Figure 1.** Location of the Pontal Sul Irrigation Scheme, Petrolina-PE, and of the agro-meteorological stations (marked in red) used to obtain climatic data.

families of small producers and rural enterprises with arable land, divided into varying sized lots: smaller lots measuring 6 ha and larger lots measuring between 20 and 40 ha (CODEVASF 2014). The orbital images used belonged to the MODIS sensor of the MOD13Q1 product, aboard the Terra platform. MOD13Q1 consists of a set of vegetation index products that generates 23 images per year, taken at 16-day intervals, with a spatial resolution of 250 m. In this study, only bands 1 and 2 were used in the visible band at reflectance level, in the h13v09 and h14v09 quadrants for the years between 2010 and 2017, with a total of 24 images.

The surface albedo ( $\alpha_0$ ) was calculated using Equation (1), proposed by Valiente et al. (1995).

$$\alpha_0 = a + b\alpha_1 + c\alpha_2 \quad (1)$$

where  $\alpha_1$  and  $\alpha_2$  are the monochromatic reflectance for bands 1 and 2 of the MODIS sensor, respectively; and  $a$ ,  $b$  and  $c$  are regression factors obtained through field data in a survey conducted by de Castro Teixeira et al. (2008) with values of 0.08, 0.41 and 0.14 for the Brazilian Semi-arid region, respectively.

The Normalized Difference Vegetation Index (NDVI) is characterized by indicating the quantity and quality of green vegetation present on the surface, and was calculated using Equation (2).

$$\text{NDVI} = \frac{\alpha_2 - \alpha_1}{\alpha_2 + \alpha_1} \quad (2)$$

where  $\alpha_1$  is the near infrared band and  $\alpha_2$  is the red band. NDVI values range from  $-1$  to  $+1$  according to vegetation characteristics.

The  $R_n$  was estimated using the Slob equation, proposed by de Castro Teixeira et al. (2008).

$$R_n = (1 - \alpha_0) \times RG - a_L \times \tau_{sw} \quad (3)$$

where  $a_L$  is the regression coefficient specified through its relationship with  $T_a$ .

$$a_L = d \times T_a - e \quad (4)$$

where  $d$  and  $e$  are regression coefficients with values of 6.99 and 39.93, respectively, for Brazilian semi-arid climatic conditions (de Castro Teixeira et al. 2013a).

Reflected short-wave solar radiation ( $RR$ ) was estimated via the product of  $\alpha_0$  and  $RG$  (de Castro Teixeira et al. 2013b), according to Equation (5).

$$RR = \alpha_0 \times RG \quad (5)$$

The atmospheric long-wave radiation ( $R_a$ ) was obtained by means of Stefan-Boltzmann's Equation (6).

$$R_a = \sigma \times \varepsilon_a \times T_a^4 \quad (6)$$

where  $\varepsilon_a$  is the atmospheric emissivity (dimensionless);  $\sigma$  is the Stefan-Boltzmann constant ( $5.67 \times 10^{-8} \text{ W m}^{-2} \text{ K}^{-4}$ ), and  $T_a$  is the air temperature in K.

Equation (7) was proposed by Bastiaanssen and Ali (2003); to determine  $\varepsilon_a$ , obtained through field experiments using alfalfa in Idaho, USA.

$$\varepsilon_a = 0.85 \times [-\ln(\tau_{sw})]^{0.09} \quad (7)$$

The  $R_s$  value was obtained using Equation (8), based on the sum of the results obtained by the difference between the  $RG$  and the  $RR$ , and by the difference between  $R_a$  and  $R_n$ , i.e. obtained as residue of the  $R_n$  equation.

$$R_s = (RG - RR) + (R_a - R_n) \quad (8)$$

The thermal bands of the MODIS image for the calculation of the surface temperature ( $T_s$ ) were not used owing to their low resolution (1000 m) and the amount of cloud coverage that hindered the study's progress. The estimation of  $T_s$  was performed as residue, according to Equation (9) (de Castro Teixeira et al. 2013b).

$$T_s = \sqrt[4]{\frac{R_s}{\varepsilon_s \times \sigma}} \quad (9)$$

where  $R_s$  is the long-wave radiation emitted by the surface, and  $\varepsilon_s$  is the emissivity of the surface, obtained through Equation (10).

$$\varepsilon_s = f \times \ln(\text{NDVI}) + g \quad (10)$$

where  $f$  and  $g$  are regression coefficients with values of 0.06 and 1.00, respectively.

For the estimation of large-scale evapotranspiration ( $ET$ ), the SAFER mathematical model was used, where it is multiplied by the grid of daily  $ET_0$  values obtained in agrometeorological stations, as described in Equation (11).

$$\frac{ET}{ET_0} = \exp \left[ h + i \times \left( \frac{T_0}{\alpha_0 \times \text{NDVI}} \right) \right] \quad (11)$$

where  $h$  and  $i$  are the specific regression coefficients for the local semi-arid conditions, with values of 1.8 and  $-0.008$ , respectively; and  $T_0$  is the surface temperature (K) (de Castro Teixeira et al. 2013b).

Biomass production (BIO) on a large scale was performed by estimating photosynthetic active radiation (PAR) by means of  $RG$  maps.

$$\text{PAR} = j \times RG \quad (12)$$

where  $j$  is the regression coefficient for Brazilian semi-arid conditions, with a value of 0.44 (Teixeira et al. 2009).

The absorbed photosynthetically active radiation (APAR) was estimated by the results of PAR.

$$\text{APAR} = f_{\text{PAR}} \times \text{PAR} \quad (13)$$

where  $f_{\text{PAR}}$  is obtained from the NDVI value according to Equation (14).

$$f_{\text{PAR}} = k \times \text{NDVI} + m \quad (14)$$

where  $k$  and  $m$  are the regression coefficients with values of 1.257 and  $-0.161$ , respectively, as described by Bastiaanssen and Ali (2003).

BIO was quantified according to Equation (15).

$$\text{BIO} = \epsilon_{\text{max}} \times E_f \times \text{APAR} \times 0.864 \quad (15)$$

where  $\epsilon_{\text{max}}$  is the maximum light use efficiency, considering a value equal to  $2.5 \text{ g MJ}^{-1}$  as the region exhibits most of the C4 species (Teixeira et al. 2009);  $E_f$  is the evaporative fraction estimated by the latent heat flux fraction ( $\lambda E$ ) by subtracting  $R_n$  and the heat flux in the soil ( $G$ ), thus transforming the  $ET$  into an energy unit.

### 3. Results and discussion

$P$ ,  $ET_0$  and  $RG$  values are shown in Figure 2 for the municipality of Petrolina, in order to better explain the evolution of  $ET$  throughout the 2010–2017 period.

The  $P$  results show that the highest rainfall volumes were concentrated between Julian Days (JD) 001 to 113 (January to April), reaching a maximum concentration with a percentage of 84.1% in 2016. According to Yan et al. (2015), a concentration of larger proportions of rainfall in the first four months of the year arises from the more meridional location of the intertropical convergence zone (ITCZ) during this time of the year, driven by the cold occurring in the North Atlantic region. Comparatively, 2013 recorded the lowest rainfall in the rainy season, with a percentage of 43.8%, lower than the percentage value of the beginning of the rainy season (November to December) of the same year, which accounted for 49% of the annual total. Droughts occurring in the middle of the rainy season are common in this region, causing damage to rainfall-dependent agriculture depending on its magnitude and duration (Muriithi 2016).

The lowest rainfall amounts were recorded in the dry season, represented by JDs 225 to 289 in 2013, with approximately 0.5% (volume of 1.4 mm) of 2013's annual total. Although 2013 exhibits significant rainfall irregularity, the lowest accumulated rainfall value belongs to 2012 – an annual total of 161.3 mm. According to Gutiérrez et al. (2014), this value

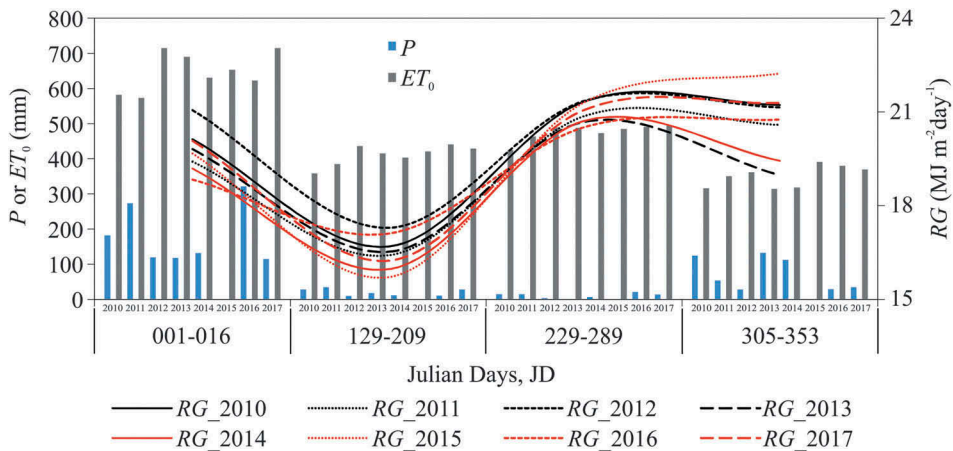


**Figure 2.** Cumulative rainfall ( $P$ ), reference evapotranspiration ( $ET_0$ ) and mean global solar radiation ( $RG$ ) values between 2010 and 2017.

stems from a variation in the Atlantic Ocean temperature caused by the Atlantic Dipole, which alters the ITCZ and results in less rainfall in the Brazilian Northeast.

$ET_0$  was higher in 2012 between JDs 001 and 113 (January to April), reaching a maximum of 714.6 mm. The high air temperatures in this season increase  $ET_0$  rates, which consequently reduces soil humidity and induces a negative climatic water balance in this region (Correia et al. 2011). The minimum recorded value was 314.1 mm for JDs 305–353 (November–December) in 2013, the start of the rainy season. According to Allen et al. (1998),  $ET_0$  variations are conditioned by meteorological factors such as air humidity, wind speed, air temperature, and solar radiation, and may vary according to characteristics of the region, such as surface cover, type of vegetation, geographic location, photoperiod, and water availability, thus affecting crop water demand planning and agricultural water usage.

The  $RG$  was high throughout the dry season (JDs 225–289) in all the years studied herein; however, the maximum average was recorded at the start of the rainy season, with a value equal to  $22.2 \text{ MJ m}^{-2} \text{ day}^{-1}$  in 2015, given the solar zenith position and the low cloud coverage conditions throughout this period in 2015. The lowest  $RG$  results were recorded at the end of the rainy season (between JDs 129 and 209), with a value of  $15.7 \text{ MJ m}^{-2} \text{ day}^{-1}$  in 2015. According to de Carvalho Alves et al. (2013), the higher the cloud cover, the lower the  $RG$  incidence on the surface, which may explain its decrease throughout and at the end of the rainy season.

Figure 3 shows the  $ET$  spatial distribution, means, and standard deviations, in terms of Julian days (JD), in the Pontal Sul Irrigation Scheme in the city of Petrolina (PE), Northeastern Brazil, for the years 2010 to 2017.

The highest  $ET$  averages were concentrated in the rainy season, where the maximum value of  $6.0 \text{ mm day}^{-1}$  was recorded in the 049–064 Julian Day (JD) interval of 2012 (between February and March), with peaks caused by rainfall accumulation (Figure 2) on previous days. de Castro Teixeira et al. (2013a), in a study of large-scale water productivity in the municipalities of Petrolina/PE and Juazeiro/BA in 2011, found that the maximum  $ET$  values are found in the rainy season, between January and April, reaching a maximum of

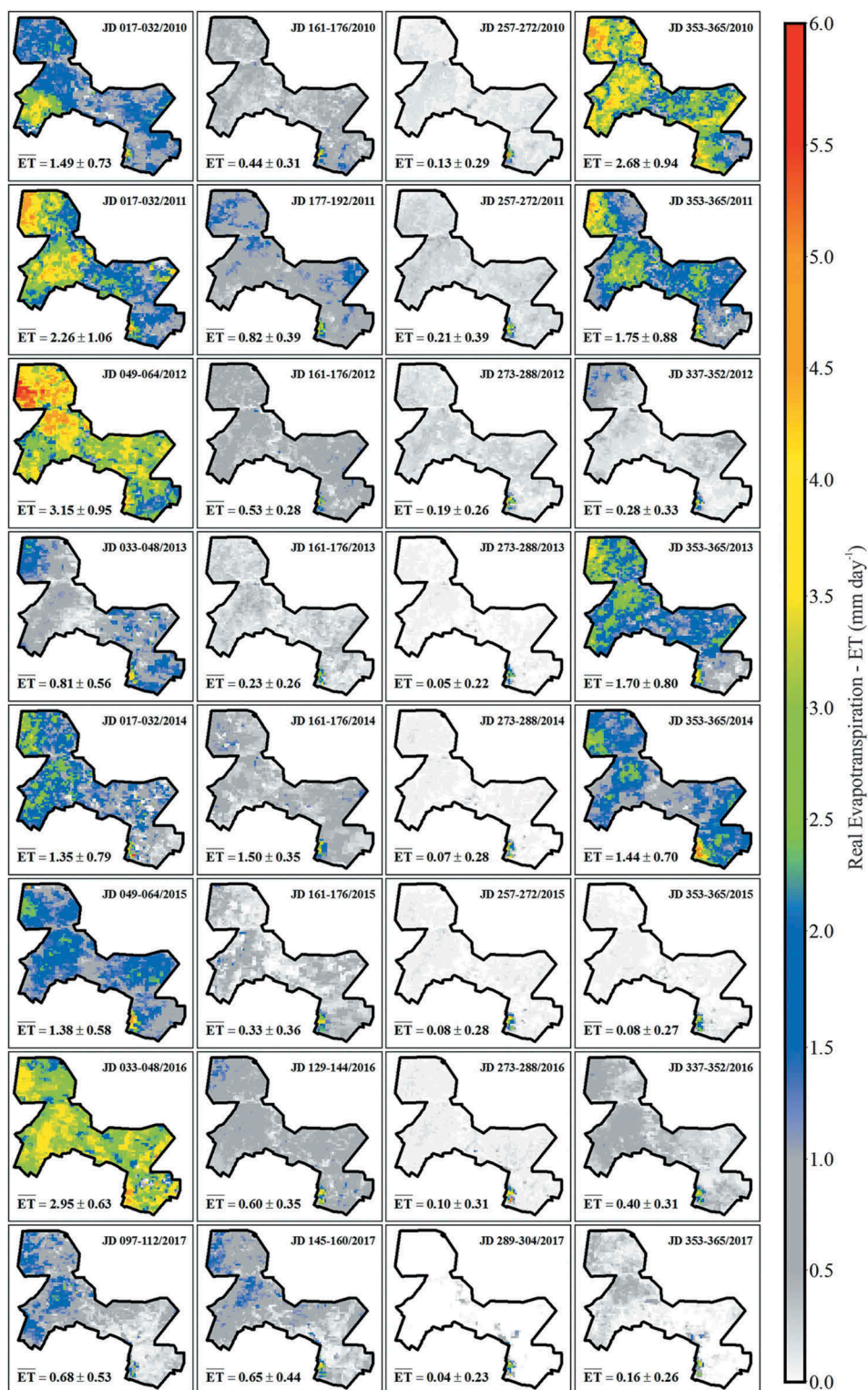


**Figure 3.** Spatial distribution of the real evapotranspiration ( $ET$ ) values, means, and standard deviations, in terms of Julian days (JD), in the Pontal Sul Irrigation Scheme, Petrolina – PE, for the 16 day periods of the MODIS product, for the years 2010–2017.

2.0 mm day<sup>-1</sup> in April. de CastroTeixeira et al. (2015) applying SAFER to Landsat-8 images to determine water productivity in 2014 in the Nilo Coelho Irrigation Scheme (located between the municipalities of Petrolina/PE and Casa Nova/BA), found a maximum result above that reported in the present work for irrigated areas 7.0 mm day<sup>-1</sup> in the rainy season. However, de Castro Teixeira et al. (2017a), using the SAFER algorithm to develop water indices in the irrigated areas of the Petrolina/PE and Juazeiro/BA agricultural regions in 2015, found results similar to the current study's for this season, with irrigated areas exhibiting maximum *ET*s of 5.40 and 4.70 mm day<sup>-1</sup>, respectively. In the Cabaceira Comprida Basin in the municipality of Santa Fé do Sul/SP, Coaguila et al. (2017) estimating *ET* by applying SAFER to Landsat-8 images in 2015, found a maximum average of 1.87 mm day<sup>-1</sup> in January, corresponding to a rainy summer. Andrade et al. (2016), applied SAFER on degraded pastures in the Alto Tocantins/GO Basin, found a maximum value of 3.4 mm day<sup>-1</sup> in 2012.

Evapotranspiration exhibited a greater heterogeneity during the rainy season – as indicated by the standard deviation (SD) data of the representative images – caused by the irregular rainfall distribution in the region. The high *ET* values in Caatinga areas occur soon after the rains, as shown in the representative rainy season images, since the preceding rainfall keeps the natural species moist and green (de CastroTeixeira et al. 2015). However, some years exhibited markedly low *ET* values during the rainy season – some close or equal to zero – due to natural phenomena that caused low *P* rates in the previous months, as seen in irrigated areas through JDs 033 to 048 in 2013 and 097 to 112 in 2017, with maximum values of 4.2 and 3.7 mm day<sup>-1</sup>, respectively.

During the years studied herein, maximum *ET* values stood out only in areas with a higher concentration of native vegetation (NV) and IA areas. However, in exposed soil regions, *ET* values were close to or equal to zero, making its variation more homogeneous, with SD ranging between 0.23 and 0.44 mm day<sup>-1</sup> between the end of the rainy season and the dry season.

The end of the rainy season presented high *ET* results, stemming from the marked accumulated *P* from the previous months. The peaks during this period also decreased, due to cloud dispersion and decreased soil moisture. The year 2014 exhibited an unusual result, with *ET* values above corresponding results for this period in the region due to a delay in the rains. On the other hand, 2013 and 2015 showed below-average results due to the low accumulation of *P* over the previous months.

Regarding the dry season, results close to or equal to zero can be found in most of the studied years. Nonetheless, the maps during this period showed points wherein *ET* is higher than the daily average, as recorded in IA areas, obtaining maximum values of 3.40 to 5.25 mm day<sup>-1</sup> in JDs 273–288 of 2013 and 2016 respectively, comprising the concentration of soil moisture retained in their root zone.

According to (de CastroTeixeira et al. 2015), due to the greater duration of drought periods in the dry season, the Caatinga vegetation uses the available energy as sensible heat flux (*H*), limiting both transpiration and photosynthesis, thus reducing *ET* values (values near or equal to zero), contrasting with the Caatinga species in irrigated areas which presented a maximum value of 5.60 mm day<sup>-1</sup>, close to the results presented in the current work. According to Teixeira and Leivas (2017), this season sees a higher atmospheric demand stimulated by the solar zenith position and low cloudiness between August and November, which causes the increase of the average *ET*<sub>0</sub> values. This increase

favours agricultural areas, where uniform crop irrigations occur daily. Sales et al. (2017) estimated the  $ET$  in a central pivot-irrigated area cultivated with tomato using SAFER at the Cabeceira do Piracanjuba farm in the municipality of Silvânia/GO, finding a maximum value of  $4.7 \text{ mm day}^{-1}$  in August (the dry season in this region).

The beginning of the rainy season yielded moderately elevated  $ET$  values, with greater heterogeneity as indicated by the SDs, where  $ET$  peaks occurred from accumulated rainfall over the previous days (Figure 2). The maximum recorded in this season occurred in 2014, with a peak of  $5.21 \text{ mm day}^{-1}$  in JDs 353 to 365, caused by the increase of irrigated areas. de Castro Teixeira et al. (2013a) registered a maximum  $ET$  value of  $200 \text{ mm month}^{-1}$  in the municipalities of Petrolina and Juazeiro between November and December 2011, corresponding to the IA areas, due to the combined effect of rainwater and irrigation usage by crops under high atmospheric demands.

Figure 4 shows the spatial distribution, means, and standard deviations of plant biomass production (BIO) in terms of JDs in the Pontal Sul Irrigation Scheme between 2010 and 2017, in Petrolina (PE), Northeastern Brazil.

Similar to  $ET$ , the highest BIO average values were found during the rainy season, where the maximum computed value reached  $287 \text{ kg ha}^{-1} \text{ day}^{-1}$  in the 16-day interval corresponding to JDs 033–048 in 2016 (in the month of February), stemming from higher soil moisture contents and  $R_G$  values in this period (Claverie et al. 2012). According to de Castro Teixeira et al. (2016), BIO production is favoured by high levels of photosynthetically active radiation (PAR) and water availability in the plants' root areas. de Castro Teixeira et al. (2013a) found the highest BIO values in the municipalities of Petrolina/PE and Juazeiro/BA between February and April, with maximum rates exceeding  $4,000 \text{ kg ha}^{-1} \text{ month}^{-1}$ , including NV and IA areas. In 2014, in the Nilo Coelho Irrigation Scheme, located between the municipalities of Petrolina/PE and Casa Nova/BA, de Castro Teixeira et al. (2015) calculated a maximum value of BIO of  $300 \text{ kg ha}^{-1} \text{ day}^{-1}$  in the areas with IA for the month of January. Teixeira and Leivas (2017), using the SAFER algorithm to determine water productivity with Landsat-8 images in the municipality of Juazeiro/BA in 2014, obtained equivalent results to those obtained here, with a maximum of  $250 \text{ kg ha}^{-1} \text{ day}^{-1}$  in IA areas. Coaguila et al. (2017) also reported high average BIO values during the rainy season in the municipality of Santa Fé do Sul/SP, reaching a maximum average of  $64.2 \text{ kg ha}^{-1} \text{ day}^{-1}$  in the month of January.

Greater heterogeneity in BIO values was found during the rainy season, as highlighted by the representative images' SDs, stemming from the irregular rainfall distribution in this region; however, over the years analysed in this study, the maximum BIO values were concentrated in areas with a greater concentration of NV and IA, whereas areas with exposed soil showed BIO results close to or equal to zero, rendering their results more homogeneous, i.e. closer to the daily average.

At the end of the rainy season, BIO values were elevated in scattered regions throughout the irrigation scheme area, with peaks occurring from the significant accumulated rainfall from the previous days and high  $ET$  averages in the irrigated areas, reaching a maximum value of  $229 \text{ kg}^{-1} \text{ day}^{-1}$  in JDs 161–176 of 2013 (month of June), even presenting the lowest recorded average among the studied years. de Castro Teixeira et al. (2015) and Teixeira and Leivas (2017) found higher averages in 2014 in the Nilo Coelho Irrigation Scheme and the municipality of Juazeiro/BA, respectively, with maximum averages of 146 and  $124 \text{ kg m}^{-2} \text{ day}^{-1}$  in IA areas.

Values close to or equal to zero were found in most of the Pontal Sul Irrigation Scheme in all studied years' dry seasons. These values arise from low accumulated  $P$  values and high  $R_G$

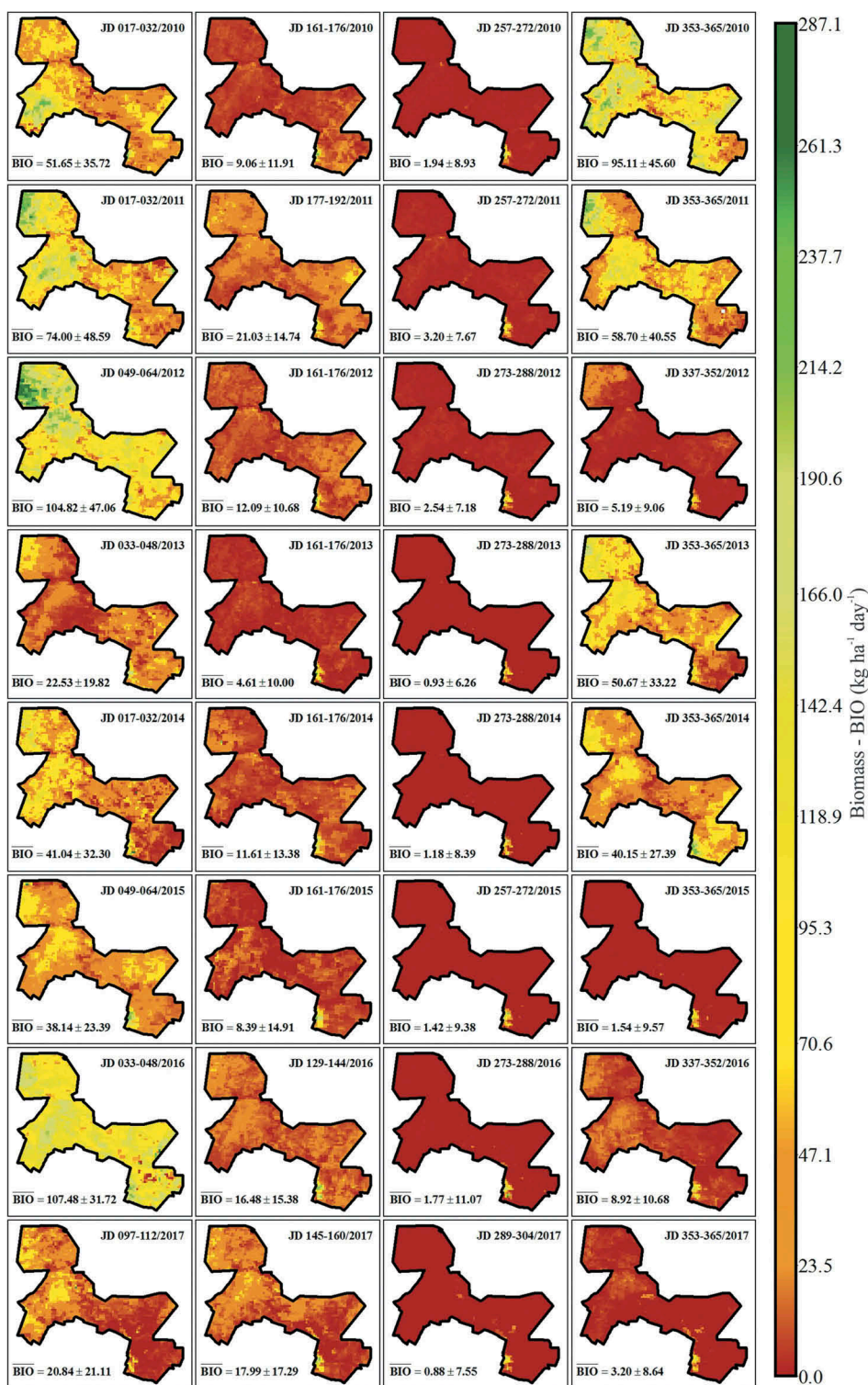


**Figure 4.** Spatial distribution of biomass values (BIO) in the Pontal Sul Irrigation Scheme, Petrolina – PE, for the 16-day period of the representative MODIS product for the years 2010 to 2017.

levels, mainly in the JDs corresponding to the months of September and October. However, in the middle of this period, there were sites within the irrigation scheme area with higher-than-average BIO values, including IA areas, with a maximum value of  $241.63 \text{ kg ha}^{-1} \text{ day}^{-1}$  in the JDs between 273 and 288 (September and October 2016), due to the concentration of moisture retained in the root zone of the plants provided by irrigation. In the municipalities of Petrolina/PE and Juazeiro/BA, de Castro Teixeira et al. (2013a) recorded the lowest results in the dry season, with pixel values around  $142$  and  $92 \text{ kg ha}^{-1} \text{ month}^{-1}$ , respectively, while de CastroTeixeira et al. (2015) found the lowest averages of BIO in the area of the Nilo Coelho Irrigation Scheme during the dry season; nonetheless, the maximum results were recorded in IA regions, where values varied between  $240$  and  $300 \text{ kg ha}^{-1} \text{ day}^{-1}$ . Likewise, Teixeira and Leivas (2017) reported that IA regions stood out in the dry season, presenting maximum results that varied between  $200$  and  $250 \text{ kg ha}^{-1} \text{ day}^{-1}$ . Andrade et al. (2016), while estimating BIO values in degraded pastures using SAFER in the Alto Tocantins/GO Basin, found maximum values of  $112.9 \text{ kg ha}^{-1} \text{ day}^{-1}$  in 2012.

Regarding the beginning of the rainy season, high average BIO values were only found in the 2010, 2011, 2013, and 2014 when compared to the rainy season, with the occurrence of peaks stemming from the considerable accumulated  $P$  over the previous days and maximum  $R_G$  averages (Figure 2). The results obtained during this season reached a maximum value of  $225.27 \text{ kg ha}^{-1} \text{ day}^{-1}$  in JDs 353–365 in 2010, corresponding to IA areas, which provided an increase in average BIO values.

#### 4. Conclusions

The use of orbital images of the MODIS sensor with the application of SAFER in conjunction with data from agro-meteorological stations provided greater detail on water demand and biomass production in the Pontal Sul Irrigation Scheme between 2010 and 2017, showing a clear difference between the rainy season, the end of the rainy season, the dry season, and the beginning of the rainy season.

Both evapotranspiration and biomass production are higher during the rainy season (comprising the months of January, February, March and April) throughout all the studied years. The irrigated agricultural area exhibited higher values than Caatinga areas, providing an increase in both evapotranspiration and biomass production, especially during the dry season.

The  $ET$  values found in Caatinga vegetation areas represent moisture in the root zone, with maximum values found during the rainy season. The biomass results are strongly influenced by water availability, as verified by the increment shown by the irrigated agricultural area when compared with the native vegetation in the irrigation scheme.

#### Acknowledgements

To the Coordenação de Aperfeiçoamento de Pessoal de Nível Superior (CAPES) for the scholarship, Embrapa's Rede AgroHidro for the support, and Embrapa Semiárido for making climatological data available.

#### Author Contributions

The authors contributed equally to the manuscript.

## Disclosure statement

No potential conflict of interest was reported by the authors.

## Funding

Coordenação de Aperfeiçoamento de Pessoal de Nível Superior (CAPES) – Financing Code 001.

## ORCID

Leandro Moscôso Araujo  <http://orcid.org/0000-0001-6621-7155>

## References

- Allen, R. G., L. S. Pereira, D. Raes, and M. Smith. 1998. "Crop evapotranspiration-Guidelines for Computing Crop Water requirements-FAO Irrigation and Drainage Paper 56." *Fao, Rome* 300 (9): D05109.
- Andrade, R. G., A. H. de Castro Teixeira, J. F. Leivas, and S. F. Nogueira. 2016. "Analysis Of Evapotranspiration and Biomass in Pastures with Degradation Indicatives in The Upper Tocantins River Basin, in Brazilian Savanna." *Revista Ceres* 63 (6) (12): 754–760. doi: [10.1590/0034-737x201663060002](https://doi.org/10.1590/0034-737x201663060002).
- Bastiaanssen, W. G., and S. Ali. 2003. "A New Crop Yield Forecasting Model Based on Satellite Measurements Applied across the Indus Basin, Pakistan." *Agriculture, Ecosystems & Environment* 94 (3): 321–340. doi:[10.1016/S0167-8809\(02\)00034-8](https://doi.org/10.1016/S0167-8809(02)00034-8).
- Claverie, M., V. Demarez, B. Duchemin, O. Hagolle, D. Ducrot, C. Marais-Sicre, J. F. Dejoux, et al. 2012. "Maize and Sunflower Biomass Estimation in Southwest France Using High Spatial and Temporal Resolution Remote Sensing Data." *Remote Sensing of Environment* 124: 844–857. doi:[10.1016/j.rse.2012.04.005](https://doi.org/10.1016/j.rse.2012.04.005).
- Cleugh, H. A., R. Leuning, Q. Mu, and S. W. Running. 2007. "Regional Evaporation Estimates from Flux Tower and MODIS Satellite Data." *Remote Sensing of Environment* 106 (3): 285–304. doi:[10.1016/j.rse.2006.07.007](https://doi.org/10.1016/j.rse.2006.07.007).
- Coaguila, D. N., F. B. T. Hernandez, A. H. D. C. Teixeira, R. A. Franco, and J. F. Leivas. 2017. "Water Productivity Using SAFER-Simple Algorithm for Evapotranspiration Retrieving in Watershed." *Revista Brasileira de Engenharia Agrícola e Ambiental* 21 (8): 524–529. doi:[10.1590/1807-1929/agriambi.v21n8p524-529](https://doi.org/10.1590/1807-1929/agriambi.v21n8p524-529).
- CODEVASF (Companhia de Desenvolvimento dos Vales do São Francisco e do Parnaíba). 2014. "Novo perímetro irrigado do Vale do São Francisco tem ritmo de implantação acelerado." Accessed 16 de August 2018. <http://www.codevasf.gov.br/principal/perimetrosirrigados/elenco-de-projetos/pontal>
- Correia, R. C., L. H. P. Kill, M. S. B. Moura, T. J. F. De, Cunha, J. Junior, and J. L. P. Araújo. 2011. *A região semiárida brasileira*, 48. Embrapa Semiárido (ALICE).
- de Carvalho Alves, M., L. Sanches, J. de Souza Nogueira, and V. A. M. Silva. 2013. "Effects of Sky Conditions Measured by the Clearness Index on the Estimation of Solar Radiation Using a Digital Elevation Model." *Atmospheric and Climate Sciences* 3 (04): 618. doi:[10.4236/acs.2013.34064](https://doi.org/10.4236/acs.2013.34064).
- de Castro Teixeira, A. H., F. B. T. Hernandez, H. L. Lopes, M. Scherer-Warren, and L. H. Bassoi. 2013b. *A Comparative Study of Techniques for Modeling the Spatiotemporal Distribution of Heat and Moisture Fluxes at Different Agroecosystems in Brazil. Remote Sensing of Energy Fluxes and Soil Moisture Content*, 1st ed., 165–187. Boca Raton, Florida: CRC Group, Taylor and Francis.
- de Castro Teixeira, A. H., J. C. Leivas, C. C. Ronquim, and D. D. C. Victoria. 2016. "Sugarcane Water Productivity Assessments in the São Paulo State, Brazil." *International Journal of Remote Sensing Applications* 6: 84–95. doi:[10.14355/ijrsa.2016.06.009](https://doi.org/10.14355/ijrsa.2016.06.009).

- de Castro Teixeira, A. H., J. F. Leivas, F. B. T. Hernandez, and R. A. M. Franco. 2017b. "Large-scale Radiation and Energy Balances with Landsat 8 Images and Agrometeorological Data in the Brazilian Semiarid Region." *Journal of Applied Remote Sensing* 11 (1): 016030. doi:10.1117/1.JRS.11.016030.
- de Castro Teixeira, A. H., J. F. Leivas, G. Bayma-Silva, and E. A. M. Garçon. 2017a. "Índices Hídricos Para Áreas Irrigadas Na Região De Desenvolvimento Agrícola Petrolina/Juazeiro." *Irriga* 1 (1): 127–135. doi:10.15809/irriga.2017v1n1p127-135.
- de Castro Teixeira, A. H., M. Scherer-Warren, F. B. T. Hernandez, R. G. Andrade, and J. F. Leivas. 2013a. "Large-scale Water Productivity Assessments with MODIS Images in A Changing Semi-arid Environment: A Brazilian Case Study." *Remote Sensing* 5 (11): 5783–5804. doi:10.3390/rs5115783.
- de Castro Teixeira, A. H., W. G. Bastiaanssen, M. U. D. Ahmad, M. D. Moura, and M. G. Bos. 2008. "Analysis of Energy Fluxes and Vegetation-atmosphere Parameters in Irrigated and Natural Ecosystems of Semi-arid Brazil." *Journal of Hydrology* 362 (1–2): 110–127. doi:10.1016/j.jhydrol.2008.08.011.
- de Castro Teixeira, A. H., J. F. Leivas, R. G. Andrade, and F. B. T. Hernandez. 2015. "Water Productivity Assessments with Landsat 8 Images in the Nilo Coelho Irrigation Scheme." *Irriga* 1 (2): 01–10. doi:10.15809/irriga.2015v1n2p01.
- de Souza, L. S. B., M. S. B. de Moura, G. C. Sediyaama, and T. G. F. da Silva. 2015. "Balanço de energia e controle biofísico da evapotranspiração na caatinga em condições de seca intensa." *Pesquisa Agropecuária Brasileira* 50 (8): 627–636. doi:10.1590/S0100-204X2015000800001.
- Gutiérrez, A. P. A., N. L. Engle, E. De Nys, C. Molejón, and E. S. Martins. 2014. "Drought Preparedness in Brazil." *Weather and Climate Extremes* 3: 95–106. doi:10.1016/j.wace.2013.12.001.
- Muriithi, F. K. 2016. "Land Use and Land Cover (LULC) Changes in Semi-arid Sub-watersheds of Laikipia and Athi River Basins, Kenya, as Influenced by Expanding Intensive Commercial Horticulture." *Remote Sensing Applications: Society and Environment* 3: 73–88. doi:10.1016/j.rsase.2016.01.002.
- Sales, D. L. A., J. Alves Junior, D. Casaroli, A. W. P. Evangelista, and J. M. F. Souza. 2017. "Estimativa de Evapotranspiração e coeficiente de cultura do tomateiro industrial utilizando o algoritmo SAFER." *IRRIGA* 22 (3): 629–640. doi:10.15809/irriga.2017v22n3p629-640.
- Shekar, N. S., and L. Nandagiri. 2016. "Actual Evapotranspiration Estimation Using a Penman-Monteith Model." *International Journal of Advances in Agricultural & Environmental Engineering* 3 (1): 161–164. doi:10.15242/IJAAEE.AE0316212.
- Teixeira, A. H. D. C. 2012. *Modelling Water Productivity Components in the Low-Middle São Francisco River Basin, Brazil. Sustainable Water Management in the Tropics and Subtropics and Case Studies in Brazil*, 1st ed., 1077–1100. Kassel: University of Kassel.
- Teixeira, A. H. D. C., and J. F. Leivas. 2017. "Determinação da Produtividade da Água com Imagens Landsat 8 na Região Semiárida do Brasil." *Conexões-Ciência e Tecnologia* 11 (1): 22–34. doi:10.21439/conexoes.v11i1.1064.
- Teixeira, A. H. D. C., W. G. Bastiaanssen, M. U. D. Ahmad, and M. G. Bos. 2009. "Reviewing SEBAL Input Parameters for Assessing Evapotranspiration and Water Productivity for the Low-Middle Sao Francisco River Basin, Brazil: Part A: Calibration and Validation." *Agricultural and Forest Meteorology* 149 (3–4): 462–476. doi:10.1016/j.agrformet.2008.09.016.
- Valiente, J. A., M. Nunez, E. Lopez-Baeza, and J. F. Moreno. 1995. "Narrow-band to Broad-band Conversion for Meteosat-visible Channel and Broad-band Albedo Using Both AVHRR-1 And-2 Channels." *Remote Sensing* 16 (6): 1147–1166. doi:10.1080/01431169508954468.
- Yan, H., W. Wei, W. Soon, Z. An, W. Zhou, Z. Liu, Y. Wang, and R. M. Carter. 2015. "Dynamics of the Intertropical Convergence Zone over the Western Pacific during the Little Ice Age." *Nature Geoscience* 8: 315–320. doi:10.1038/ngeo2375.